26th IAEA Fusion Energy Conference, Kyoto, Japan Oct 17-21, 2016

Laser-driven ion acceleration on LFEX for fast ignition: State of the art and applications

Akifumi YOGO

Institute of Laser Engineering (ILE), Osaka University, Japan

OSAKA UNIVERSITY ILE OSAKA KPSI Kansai Photon Science Institute LHD NIFS ILT Institute for Laser Technology GPI

Institute of Laser Engineering, Osaka University

N. Iwata, A. Morace, Y. Arikawa, S. Fujioka, S. Tosaki, T. Ikenouchi, K. Matsuo, T. Gawa, Y. Taguchi, S. Sakata, S. Kojima, S-H. Lee, H. Nagatomo, H. Nihsimura, M. Nakai, H. Shiraga, Y. Fujimoto, K. Yamanoi, T. Norimatsu, S. Tokita,Y. Nakata, T. Jitsuno, J. Kawanaka, N. Miyanaga, LFEX laser group, and H. Azechi

Kansai Photon Science Institute, QST

A. Sagisaka, K. Ogura, M. Nishikino, S. V. Bulanov, A. S. Pirozhkov, T. Zh. Esirkepov, and K. Kondo

Hiroshima University

T. Johzaki

National Institute for Fusion Science

T. Ozaki and H. Sakagami

Institute of Laser Technology

A. Sunahara

Institute of Physics, Chinese Academy of Sciences

Z. Zhang

The Graduate School for the Creation of New Photonics Industries

K. Mima

LFEX at ILE

Fusion fast ignition driven by ions.

Laser-accelerated protons as an alternative igniter

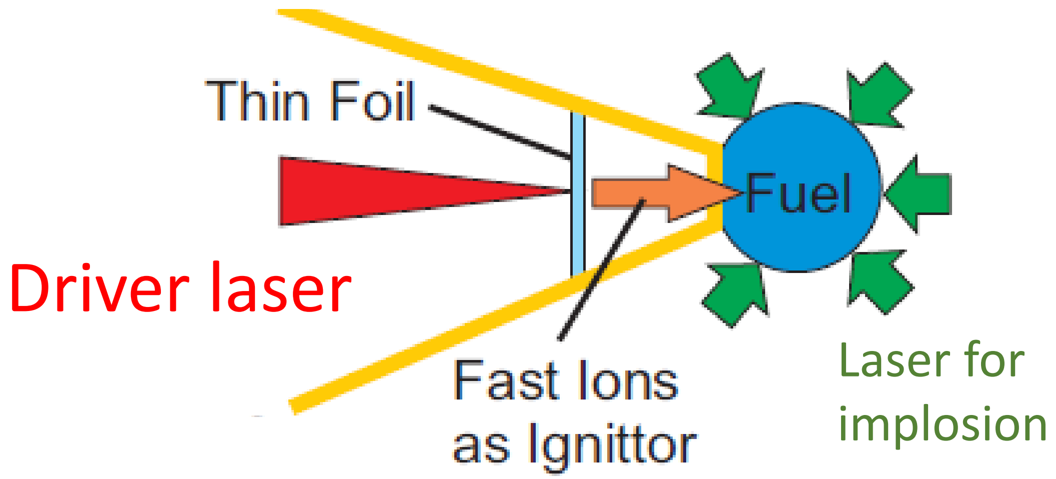

10 kJ ion-energy deposition onto the ~500 g/cm^3 fuel

100 kJ is the technically manageable energy of the driving laser

Energy conversion efficiency

$$= \frac{\text{Kinetic energies of ions having 10-30 MeV/u}}{\text{Energy of driver laser}} \geqq 10\%$$

Fernandez et al., Nucl. Fusion 49 (2009) 065004

Fusion fast ignition driven by ions.

Laser-accelerated protons as an alternative igniter

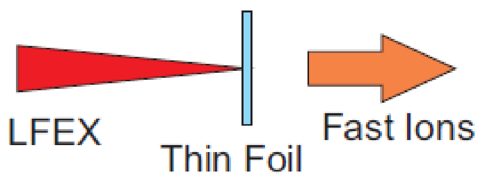

STEP 1

Ion acceleration test

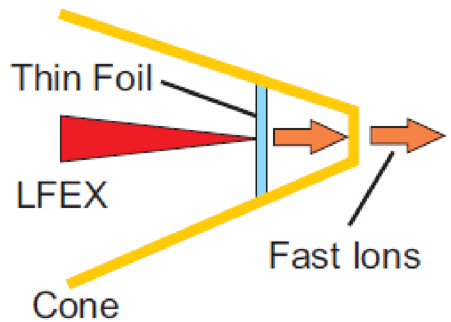

STEP 2

Ion delivery test

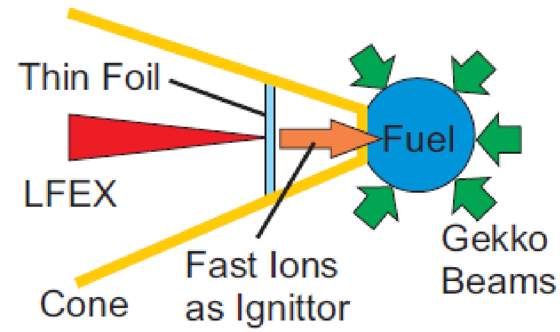

STEP 3

Ion driven Fast Ignition

Fusion fast ignition driven by ions.

Laser-accelerated protons as an alternative igniter

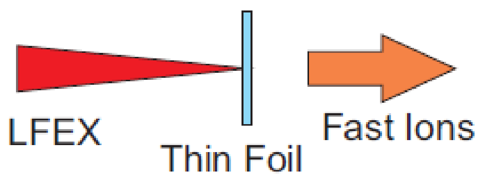

STEP 1

Ion acceleration test

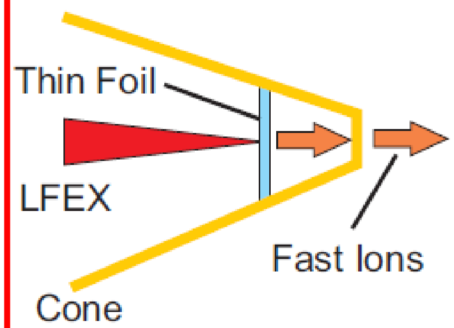

STEP 2

Ion delivery test

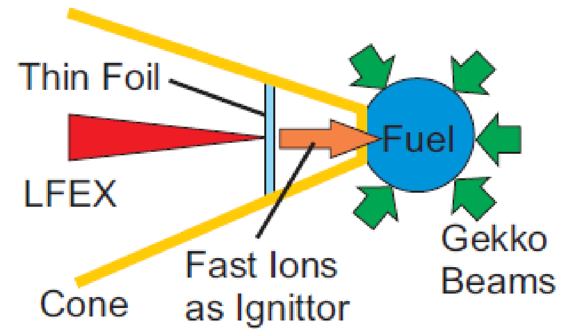

STEP 3

Ion driven Fast Ignition

To improve ion energy
and
conversion efficiency

THIS WORK

Newly developed scheme

Temporally evolution of electron temperature in pico-second region

Summary of Achievement

30 MeV proton generation with 5% conversion efficiency

LFEX

kJ, ps, High-contrast laser

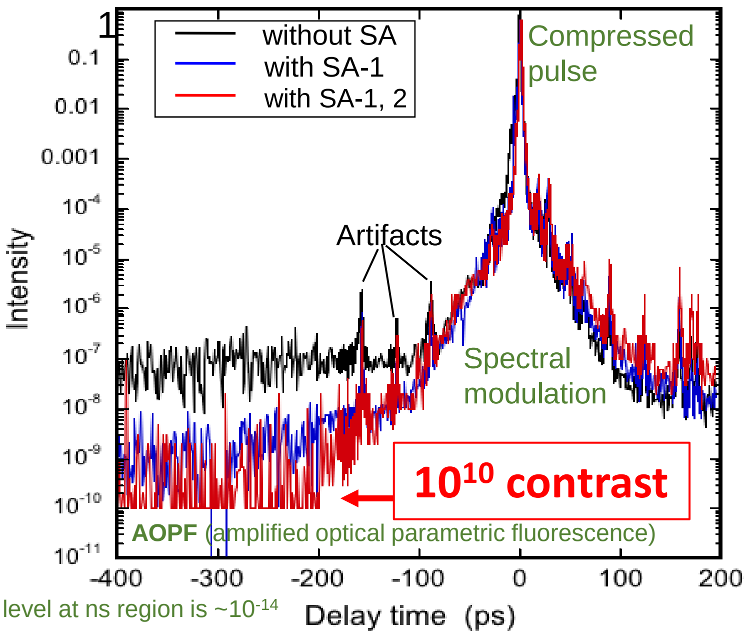

ASE level at ns region is ~10^{-14}

World highest achievement as kJ laser

30 MeV on ion kinetic energy

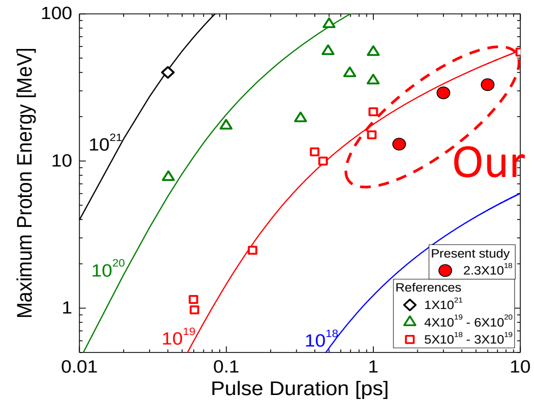

5% on energy-conversion eff.

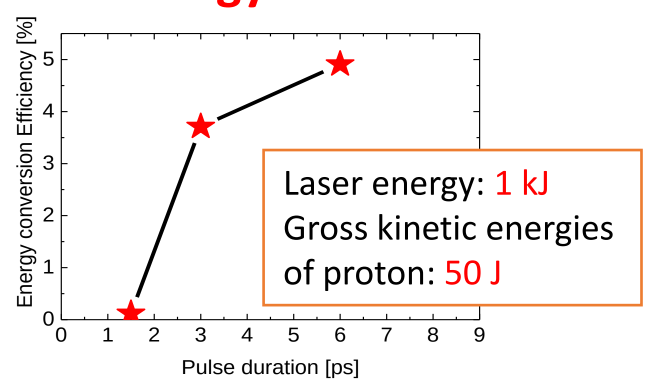

We have achieved these results with 10^{18} $\mathrm{Wcm^{-2}}$ laser intensity.

c.f. In previous works, similar results were obtained with $10^{19\text{-}20}$ $\mathrm{Wcm^{-2}}$ lasers.

Ion acceleration with 10^{18}-10^{20} Wcm^{-2} laser intensity

TNSA model: ion acceleration from the target rear surface.

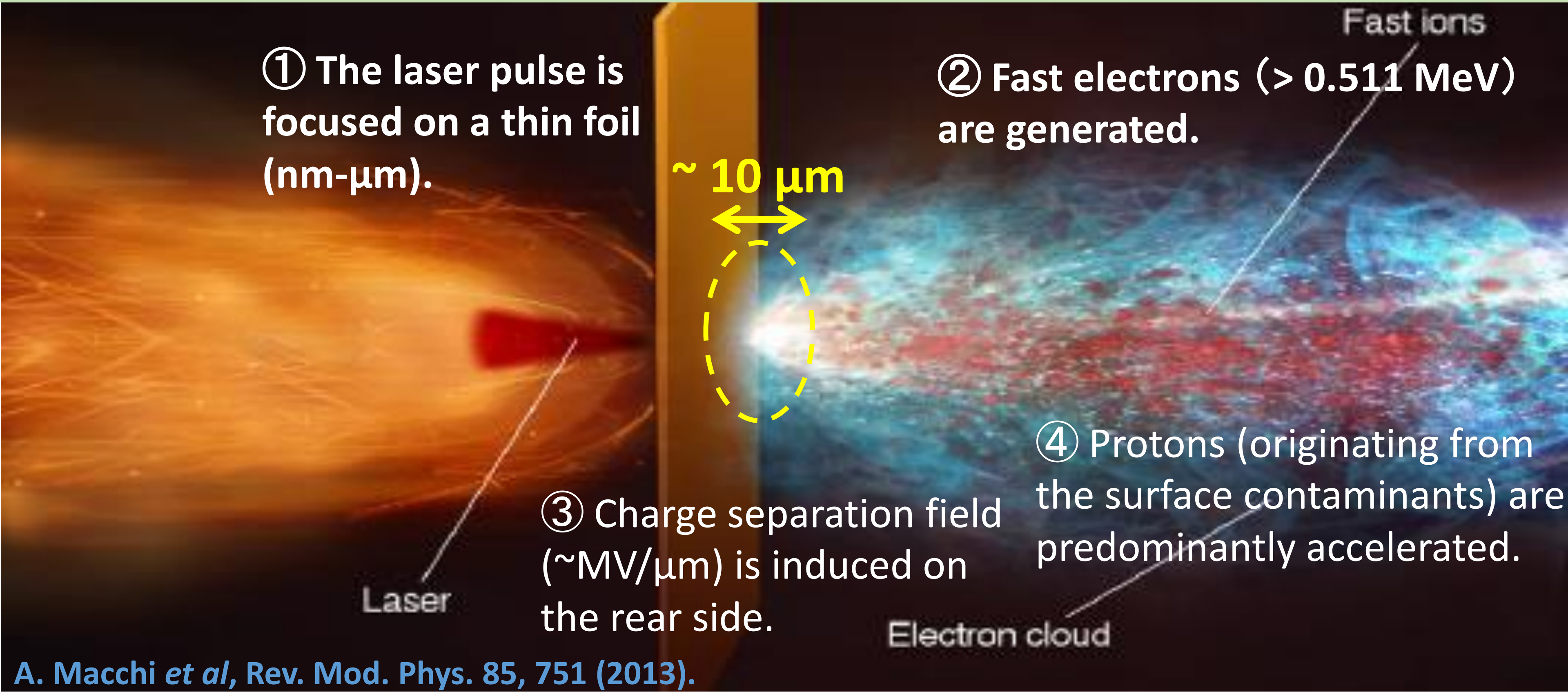

A. Macchi *et al*, Rev. Mod. Phys. 85, 751 (2013).

Maximum ion energy predicted by 1 dimensional (1D) isothermal model

$$\boxed{\mathcal{E}_{max} = 2T_h\left[\ln\left(t_p + \sqrt{t_p^2+1}\right)\right]^2}$$

P. Mora Phys. Rev. Lett. **90**, 185002 (2003)

In this model, the electron temperature is never evolved as time.

Experimental conditions

Ion energy distributions are measured at the rear side of thin-foil targets.

LFEX: ps laser

1.5 ps, 1 kJ on target
1.2×10^{19} Wcm^{-2}
60 µm spot (FWHM)
4 beams in total.

The arrival timing of 4 LFEX beams can be set independently of each other.

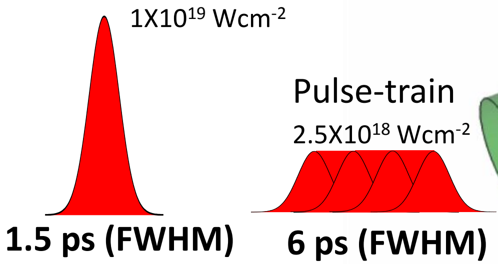

Thin-foil target

5 or 10-µm-thick AL

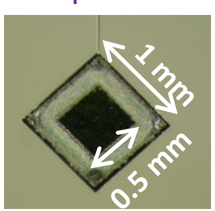

Spot size >> target thickness
(60 µm) (5-10 µm)

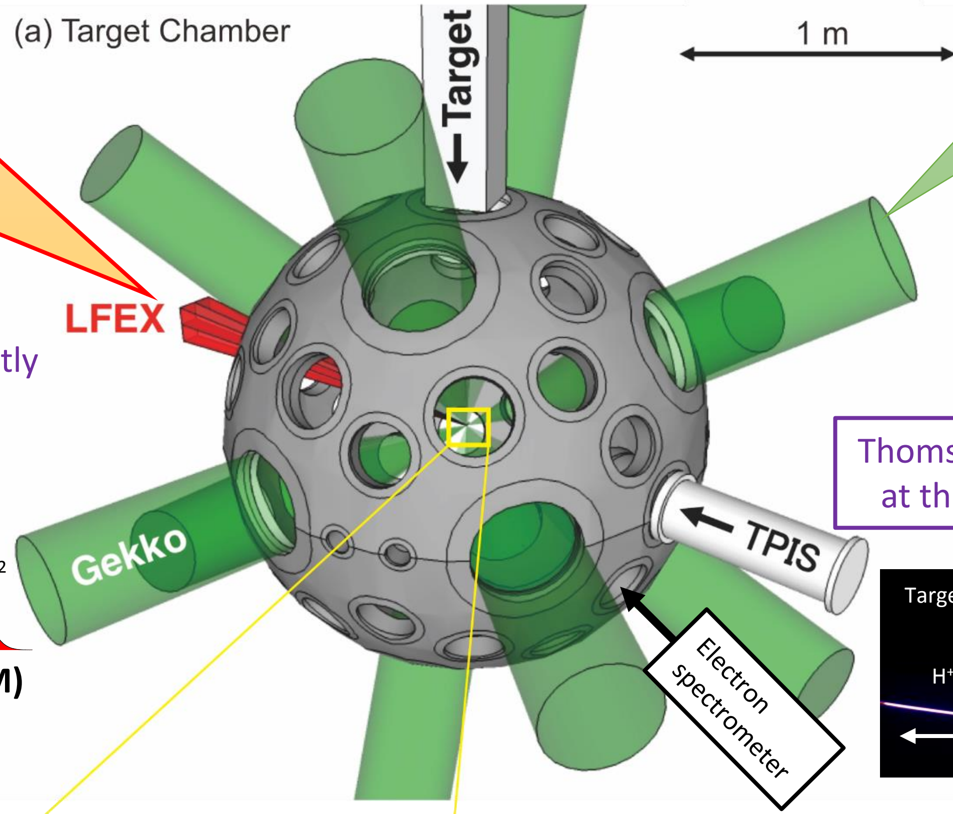

Gekko-XII: ns laser for fuel implosion 12 beams in total.

Thomson parabola Ion spectrometer at the laser propagation direction

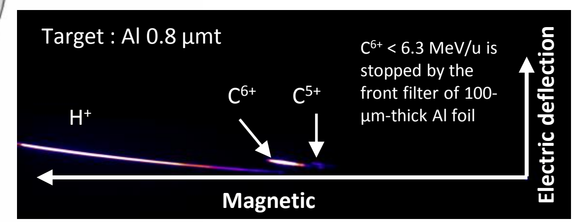

Electron energy spectra are measured simultaneously with ions.

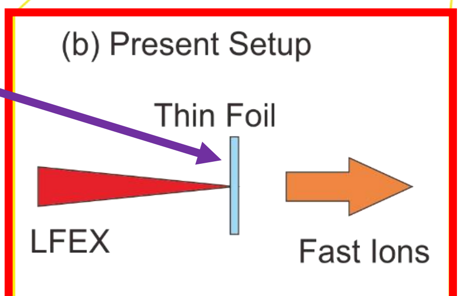

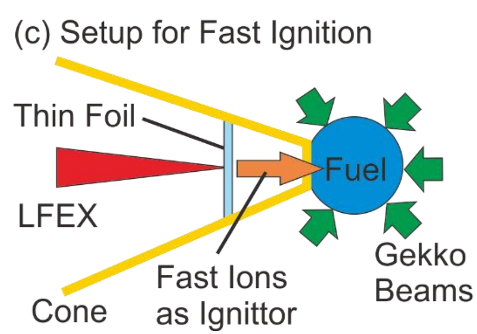

ILE OSAKA

Proton energy increases with the pulse duration.

Our experimental results clearly exceed the prediction of usual model.

【Pulse duration】

1.5 ps	⇒	3 ps	⇒	6ps
1 pulse		2-pulse train		4-pulse train

The intensity is fixed on $2.3 \times 10^{18}\ Wcm^{-2}$

Our proton energy is close to 10^{19} Wcm^{-2} line by results of conventional lasers.

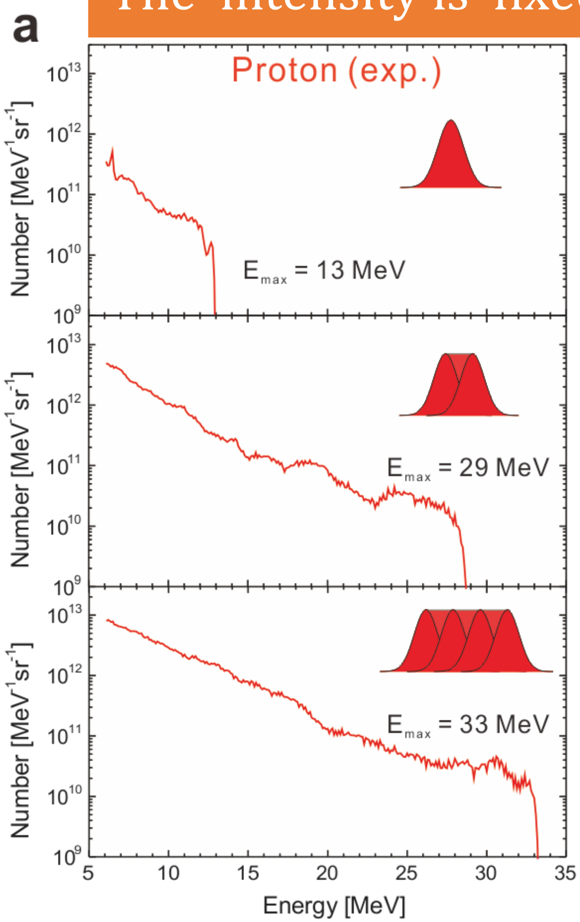

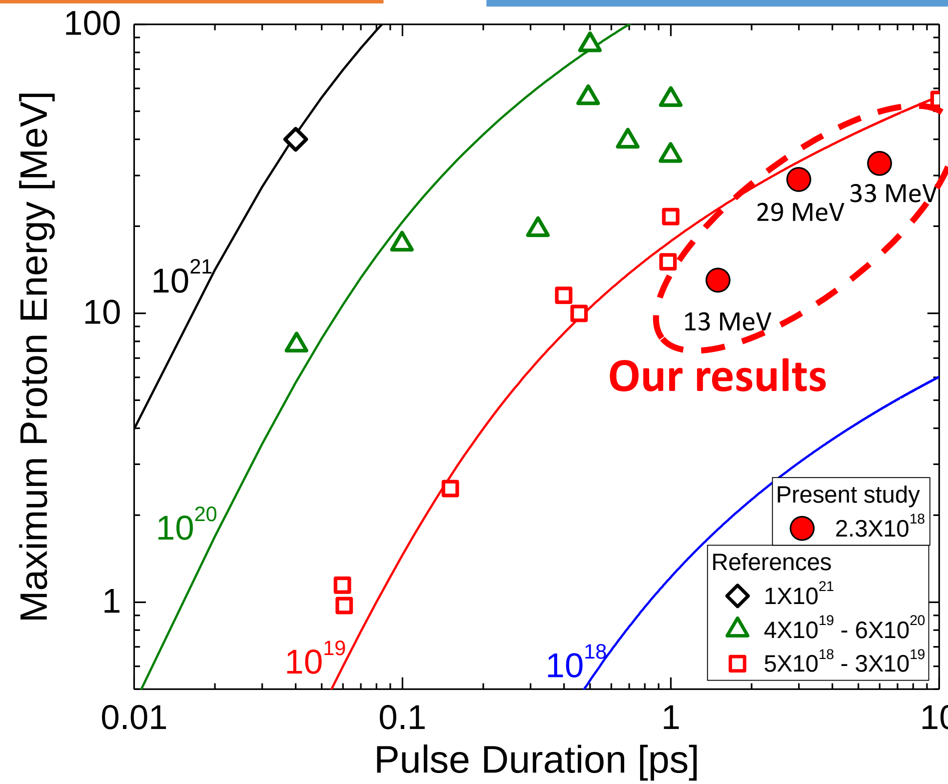

Fuchs, J. *et al.* Laser-driven proton scaling laws and new paths towards energy increase. *Nat. Phys.* **2**, 48-54 (2006).

Conversion Eff. increases with the pulse duration.

【Pulse duration】

1.5 ps	⇒	**3 ps**	⇒	**6ps**
1 pulse		2-pulse train		4-pulse train

The intensity is fixed on $2.3 \times 10^{18}\ Wcm^{-2}$

Similar efficiency was obtained with 10^{20} Wcm^{-2} conventional lasers.

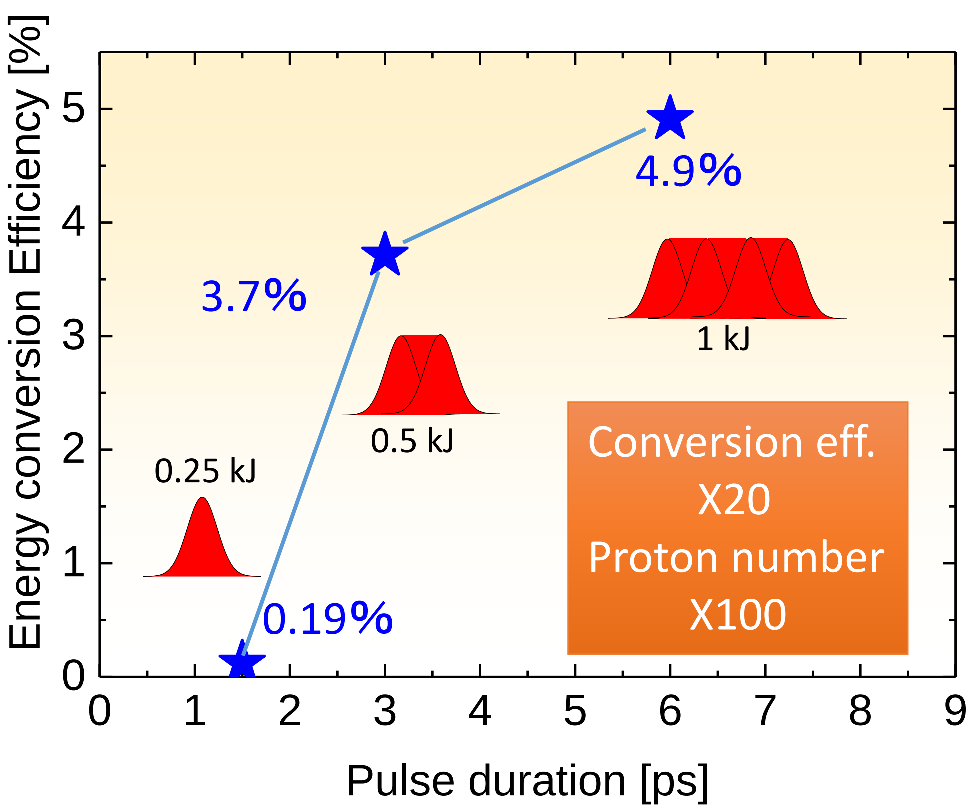

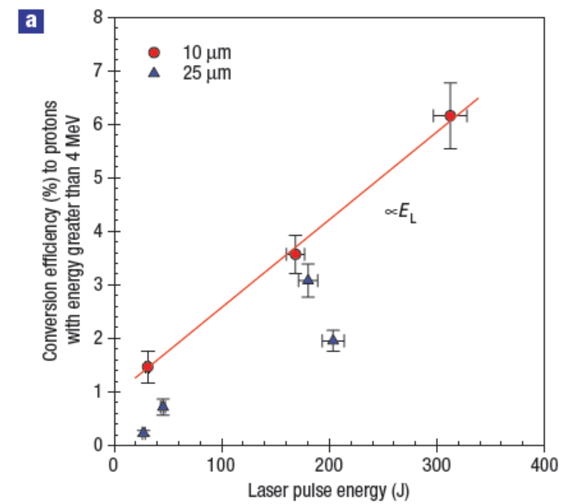

6% Conversion Eff. was obtained with 6×10^{20} Wcm^{-2}

Robson, L. et al Nat. Phys. 3, (2007).

Energy conversion efficiency

$$= \frac{\text{Kinetic energies of ions}}{\text{Laser energy}}$$

Electron temperature increases with pulse duration.

The temperature exceed a usual scaling law.

【Pulse duration】

1.5 ps	⇒	3 ps	⇒	6ps
1 pulse		2-pulse train		4-pulse train

The intensity is fixed on 2.3×10^{18} Wcm^{-2}

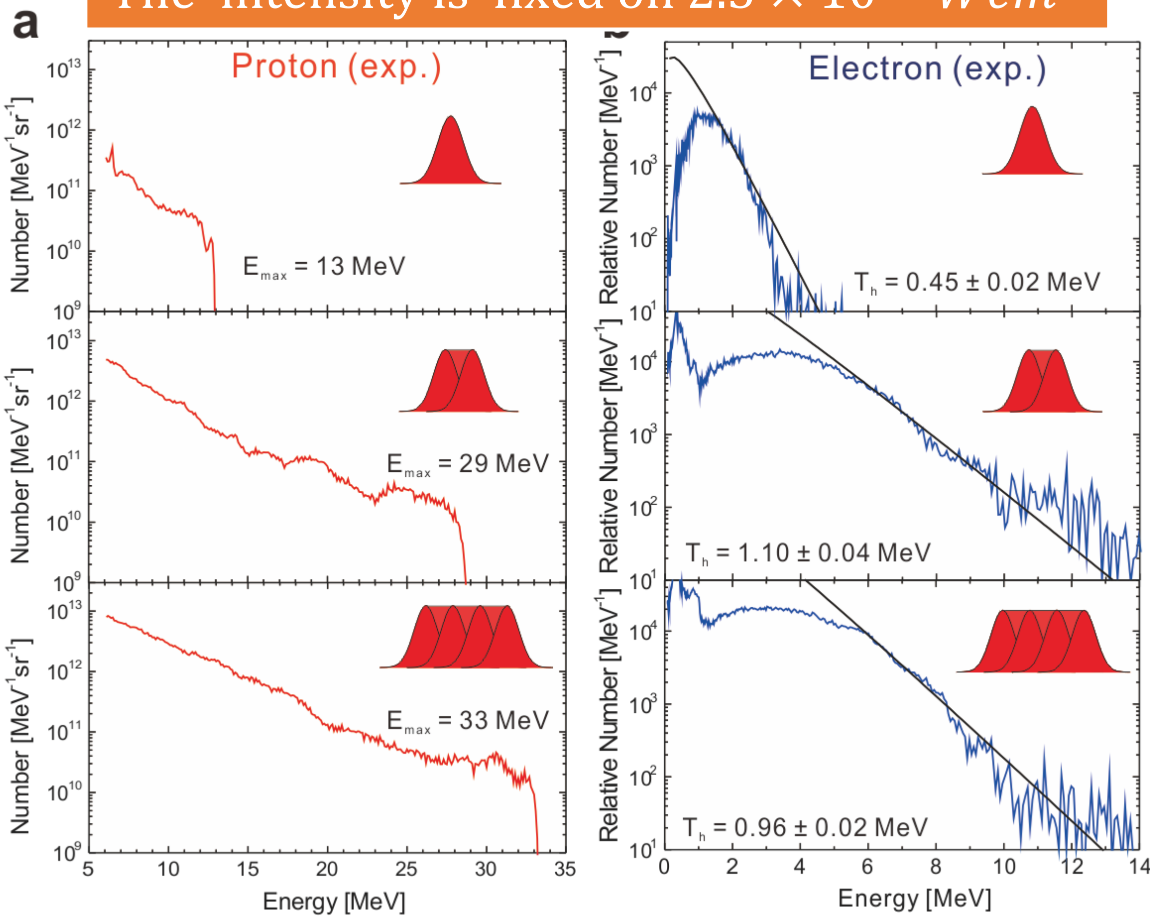

Conventional scaling law

Ponderomotive energy

$$\boxed{T_0 = m_e c^2(\gamma - 1)}$$

Wilks et al., PRL 96, 13831992

$$\gamma = \sqrt{1 + a_0^2/2}$$

$$a_0 = 0.85\sqrt{I[Wcm^{-2}]\lambda^2[\mu m]/10^{18}}$$

$T_0 = 0.2$ MeV

for $I = 2.3 \times 10^{18}$ Wcm^{-2}

(No time dependency)

However, in our experiment,

0.45 ⇒1.10 ⇒ 0.96 MeV

Never explained by the ponderomotive scaling

Comparison btw experiment and PIC simulation

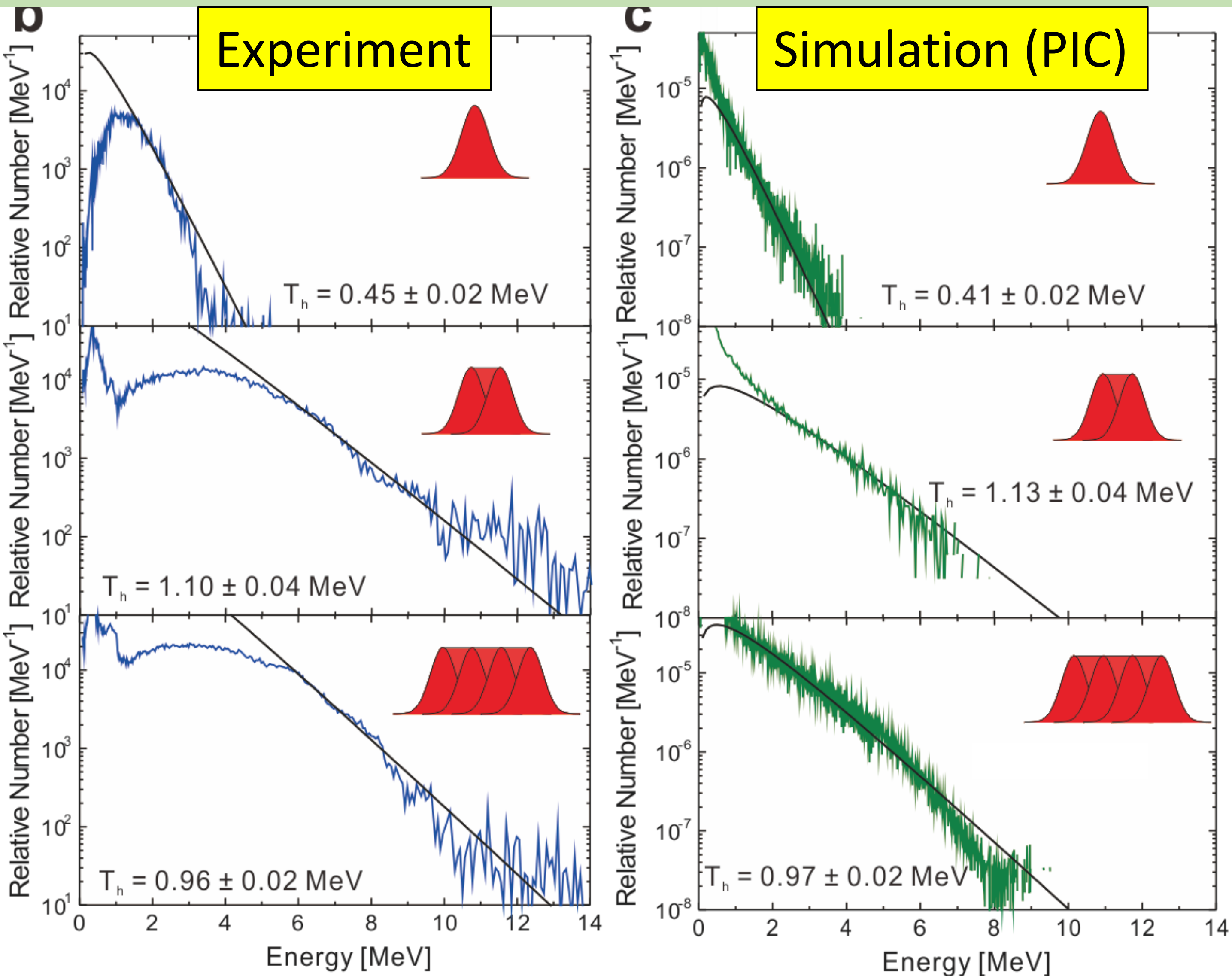

The PIC results quantitatively agree with the experiments

Mechanism underlying the heating

Electrons are heated during recirculating the target.

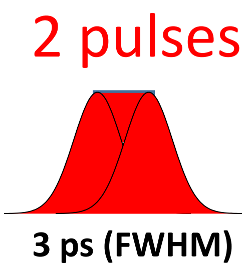

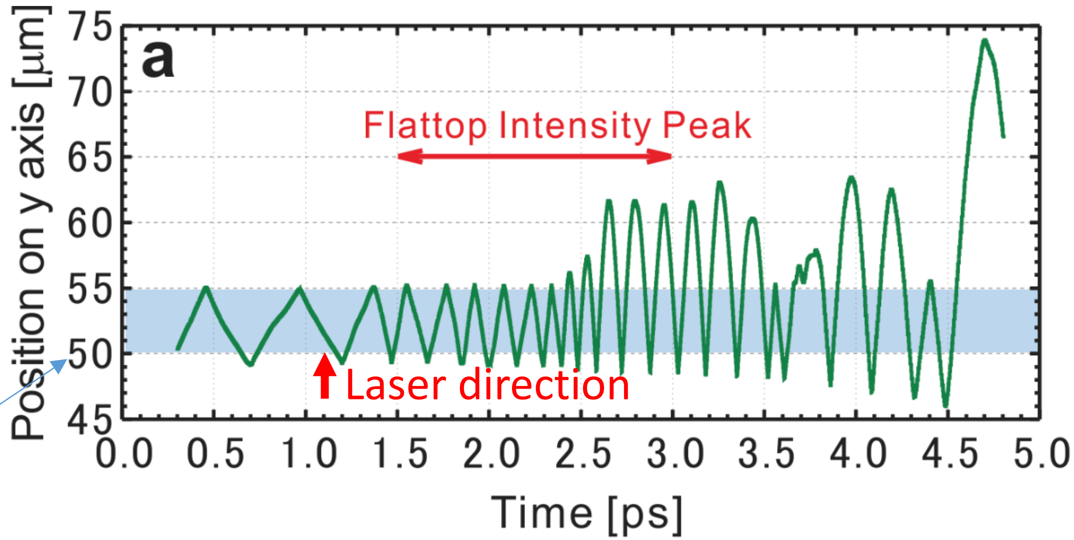

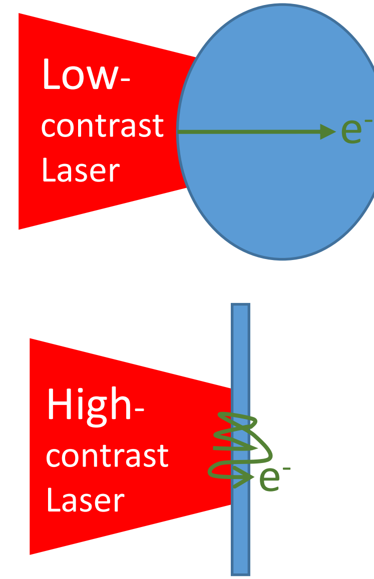

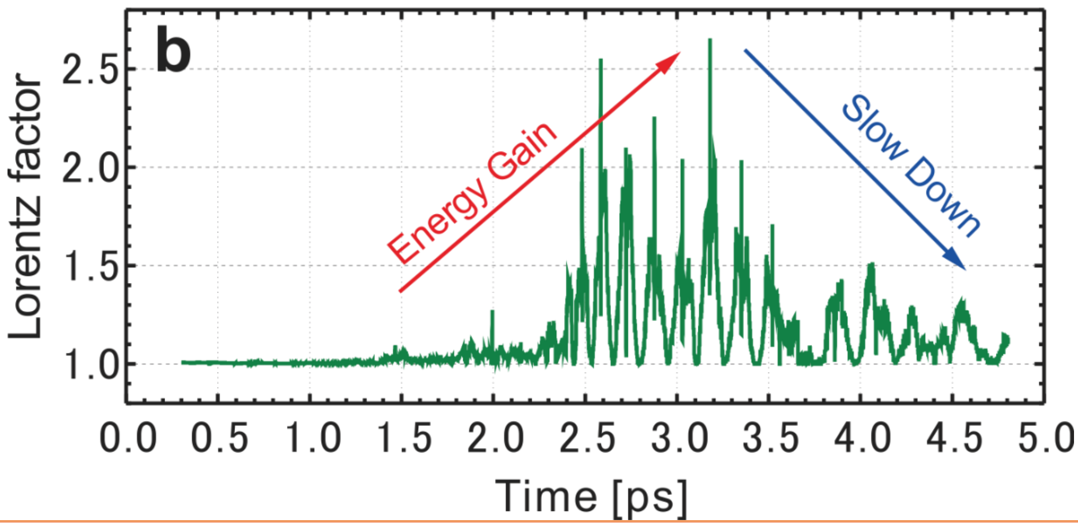

When the laser is incoming, electrons are accelerated forward and reflected by the charge-separation field on the rear side and go back to the front side. Then, again kicked by the laser. The electron's energy increases stochastically during the laser pulse duration.

The electron motion above never happens when a seriously large plasma expansion is made by low-contrast laser.

We introduce the temporally evolved temperature into analytical model, based on self-similar solutions.

$$n_e = n_{e0} \exp\left(e\phi/T(t)\right),$$
$$\epsilon_0 \partial_x^2 \phi = e(n_e - Z n_i),$$
$$\partial_t n_i + \partial_x (n_i v_i) = 0,$$
$$\partial_t v_i + v_i \partial_x v_i = -Ze\partial_x \phi / m_i,$$

We newly introduce time dependency onto the self-similar variable

$$\boxed{\xi = \frac{x}{R(t)}, \quad R(t) = \int_0^t c_s(t')dt',}$$

Ion acoustic velocity <u>depending on time</u>

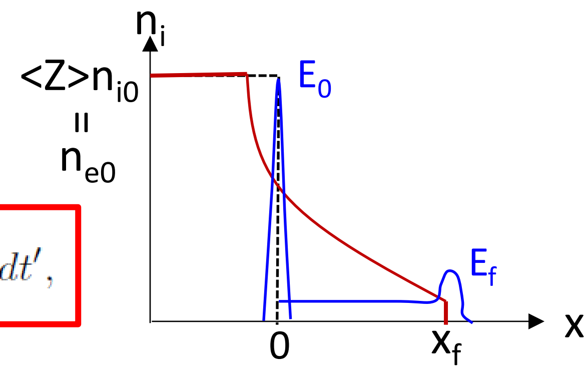

Self-similar solution of the electric field

$$e\phi = -T(t)(\xi + 1)$$
$$E_{ss} = -\partial_x \phi = T(t)/eR(t).$$

Electric field on the ion front Assumed by Mora

$$\boxed{E_f(t) \simeq 2E_{ss} = \frac{2T(t)}{eR(t)}.}$$

Ponderomotive energy

<u>Norimarization</u> $\tau = \omega_{pi0} t/\sqrt{2e_N}, \quad \bar{c_s}^2(\tau) = T(\tau)/T_0.$

Ion velocity at the front

$$v = 2c_{s0} \int \frac{\bar{c_s}^2(\tau)}{\sqrt{1 + R^2(\tau)}} d\tau, \qquad c_{s0} = \sqrt{ZT_0/m_i}$$

Ion kinetic energy at the front

$$\boxed{\mathcal{E} \simeq \frac{1}{2} m_i v^2 = 2T_0 \left[\int \frac{\bar{c_s}^2(\tau)}{\sqrt{1 + R^2(\tau)}} d\tau \right]^2}$$

ILE OSAKA

Maximum proton is analytically reproduced.

We find a fairly well agreement with the experiments.

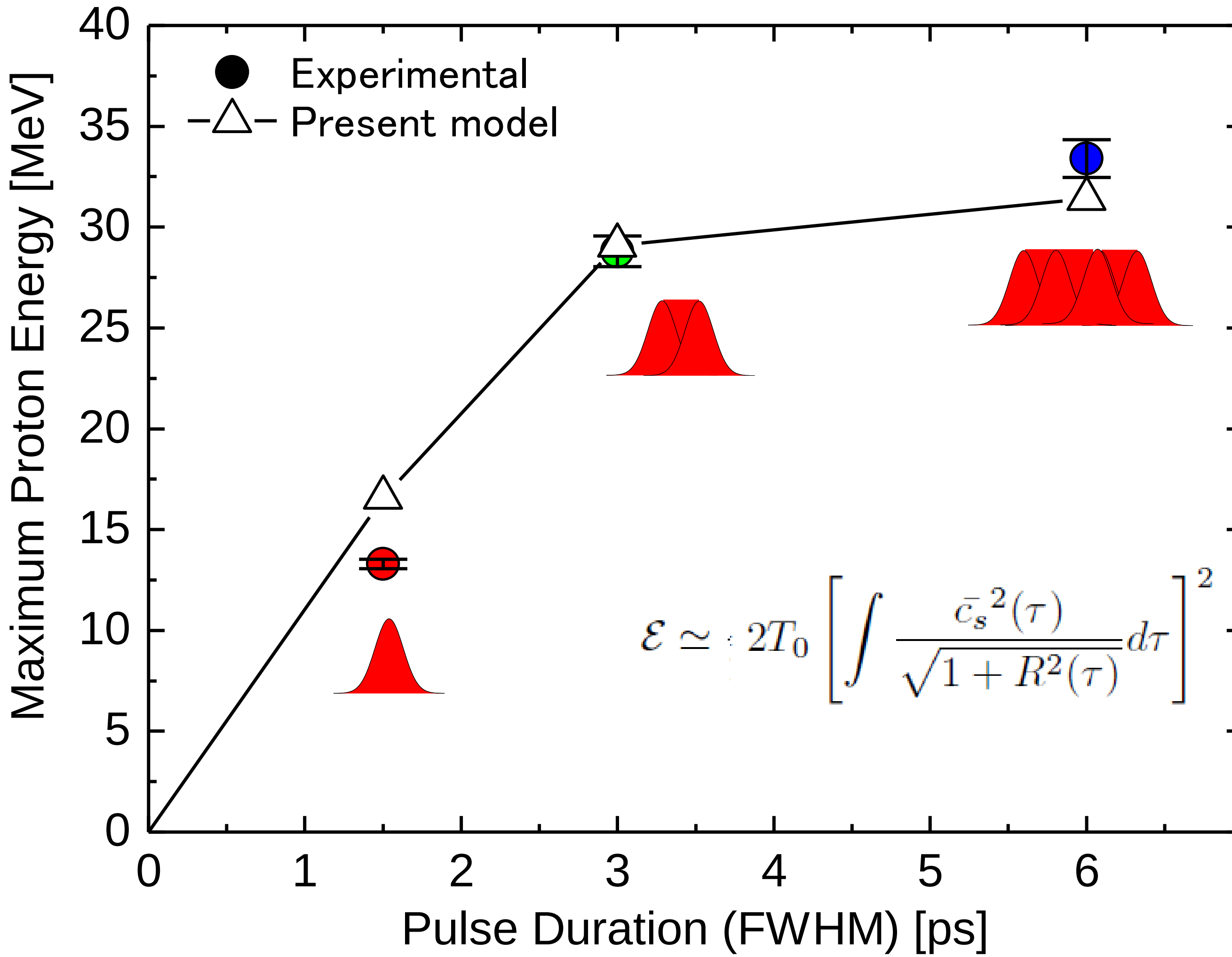

The temporal evolution of electron temperature enables to improve proton energy up to 30 MeV.

ILE OSAKA

Energy absorption into ions increases as time in PIC.

Simulation (PIC)

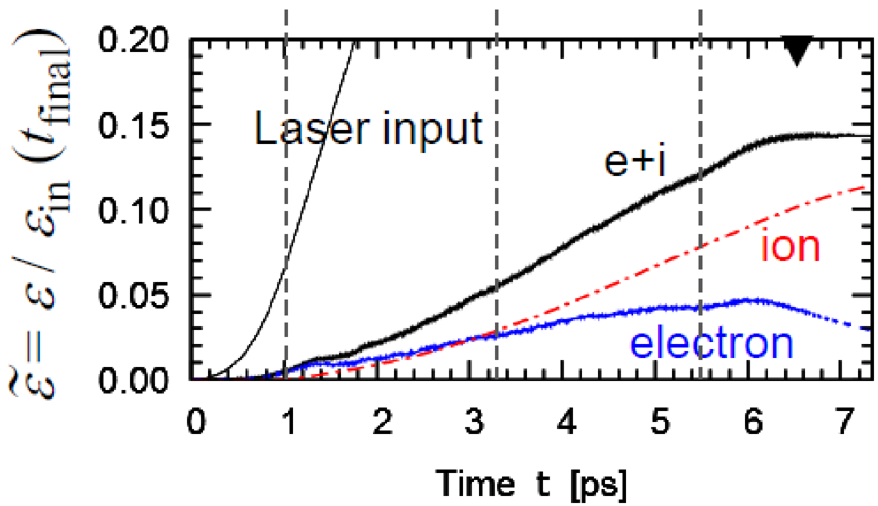

Experiment

Ion (conversion eff.)

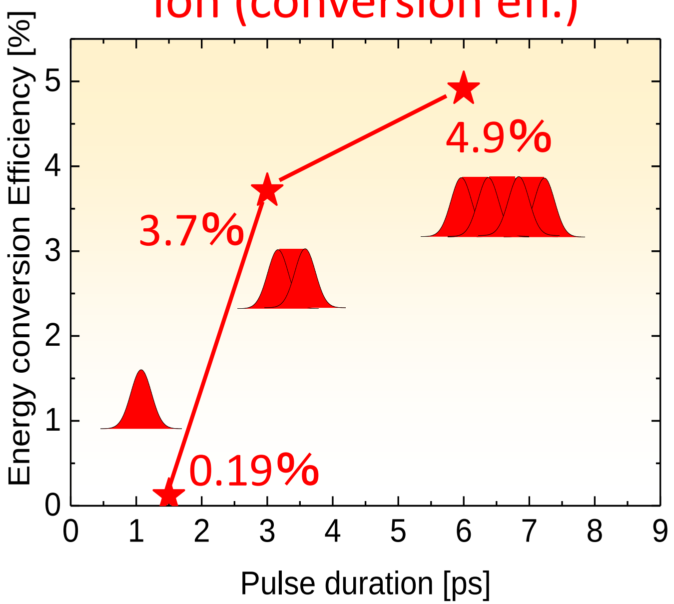

The PIC simulation qualitatively predicts the temporal evolution of the conversion eff.

The temporal evolution of electron temperature enables to improve conversion eff. up to 5%.

Conclusion

THIS WORK

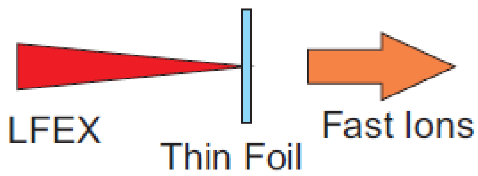

STEP 1

Ion acceleration test

30 MeV protons with 5% conversion eff. with the temporally-evolution effect.

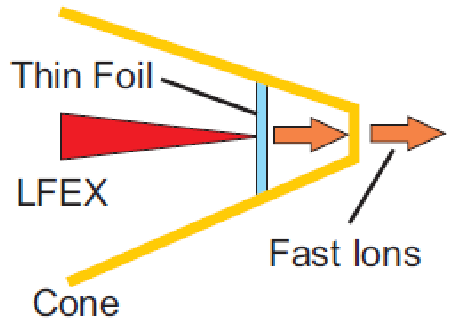

STEP 2

Ion delivery test

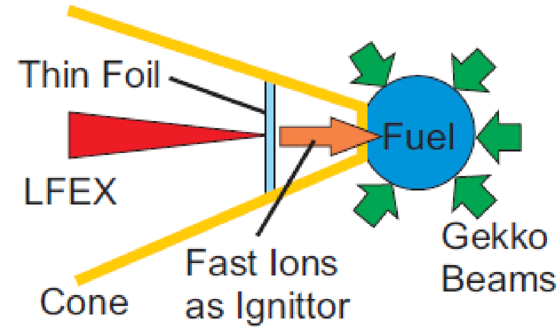

STEP 3

Ion driven Fast Ignition

Final requirement

30 MeV, ≧10% with 100 kJ laser

Conclusion

ILE OSAKA

THIS WORK

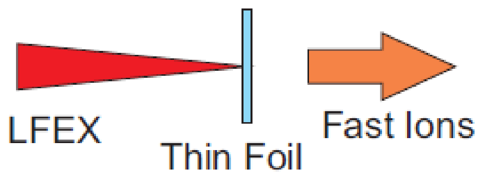

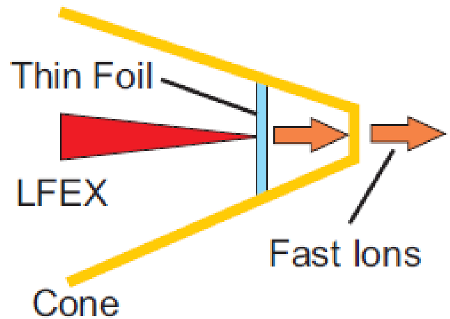

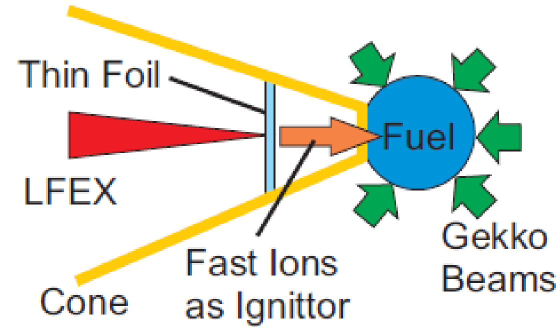

<u>STEP 1</u>

Ion acceleration test

30 MeV protons with 5% conversion eff. with the temporally-evolution effect.

<u>STEP 2</u>

Ion delivery test

STEP 3

Ion driven Fast Ignition

To achieve the requirement, we find the upper limit of the temporally evolution in a few 10s ps region, accompanied with the upgrade of LFEX laser.

<u>Requirement</u>

30 MeV, ≧10% with 100 kJ laser

The focal spot (60 μm) in our experiment leads to 1D plasma expansion.

We try to explain the experimental results using 1D PIC simulation.

We have to evaluate the electron heating in the region up to 10 ps for the 4-pulse train case.

2D PIC simulation in the multi-ps time scale is time consuming, almost impossible.

We find that when the focal spot is set to be 60 μm, the 2D PIC results are well in agreement with the results obtained in 1D simulation, in the case of 1.5 ps pulse duration.

We evaluate the electron heating in multi-ps region by using 1D PIC simulation that probably reproduces the condition of actual experiment.

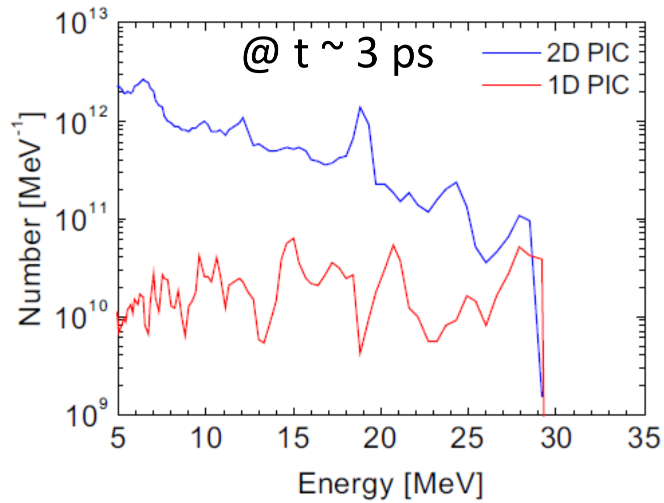

Proton energy spectra obtained with 2D PIC simulation assuming a 60 μm focal spot (blue) and 1D PIC (red). The laser pulse has 1.5 ps duration and 1X10^{19} Wcm^{-2} intensity.

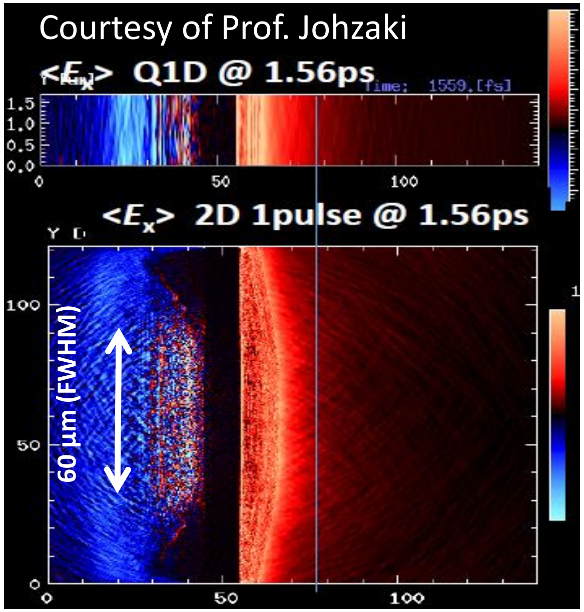

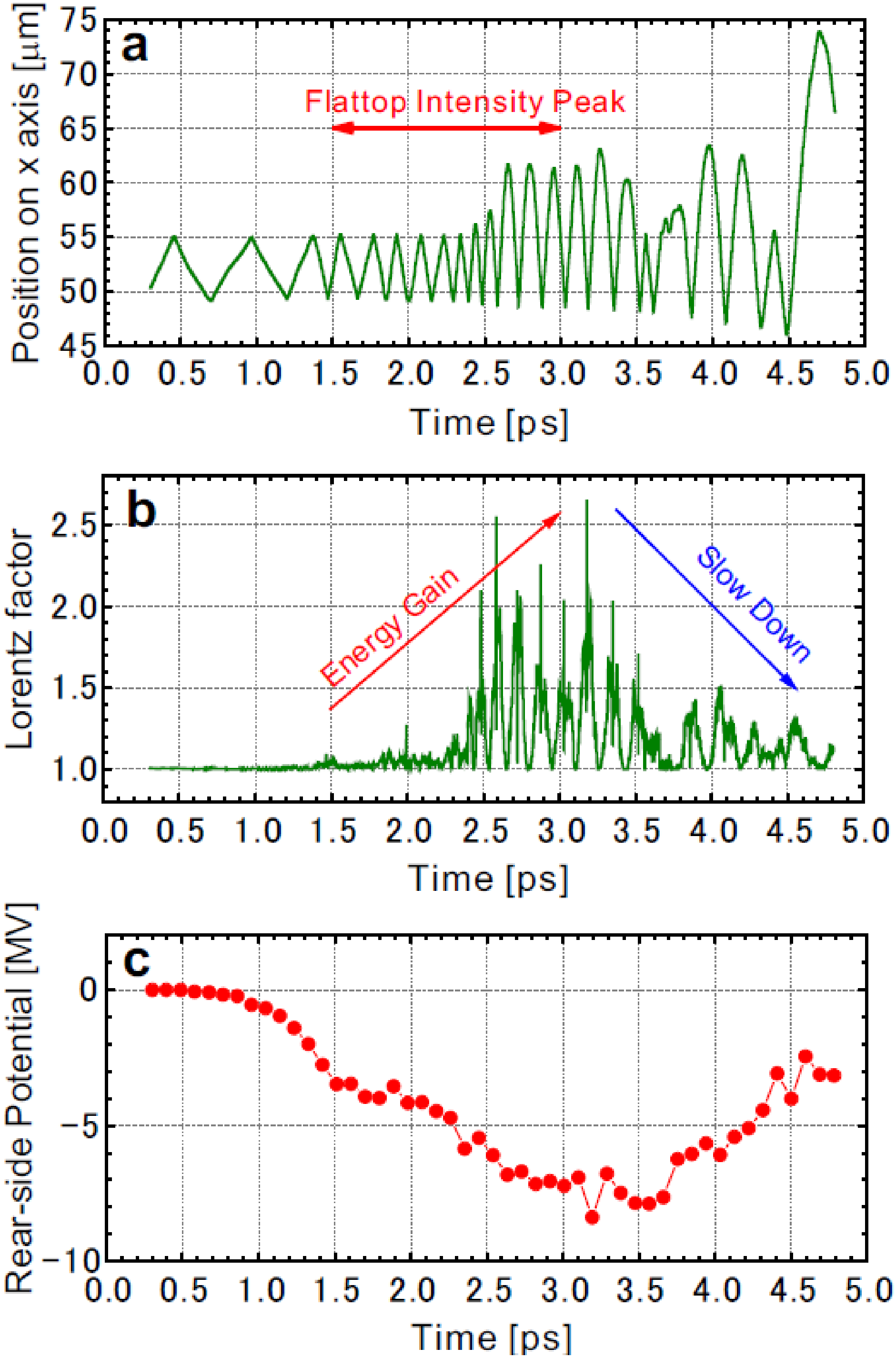

FIG. 3. (a) Trace of typical electron trajectory in the 1D PIC simulation. The target foil is initially at the position $x = 50$-55 μm and the laser (2-pulse train) is incident on the surface at $x = 50$ μm. (b) Time evolution of the Lorentz factor of the electron shown in (a).

Results 

シミュレーション結果：電子・イオンエネルギー時間発展と相互作用の様子

エネルギー密度（吸収率）の時間発展

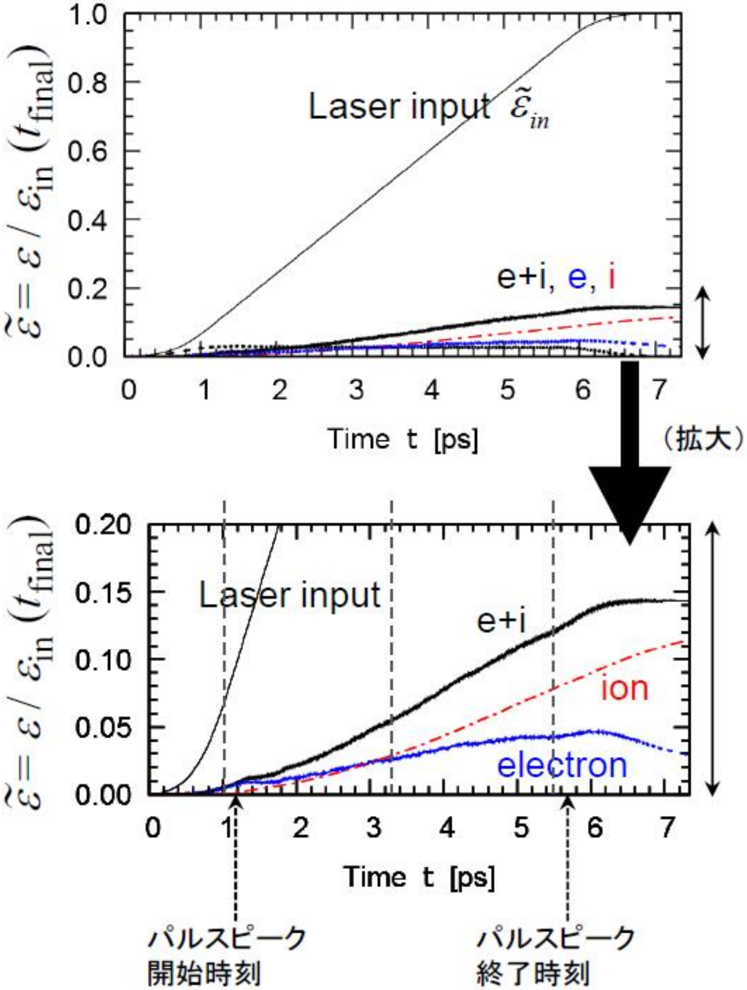

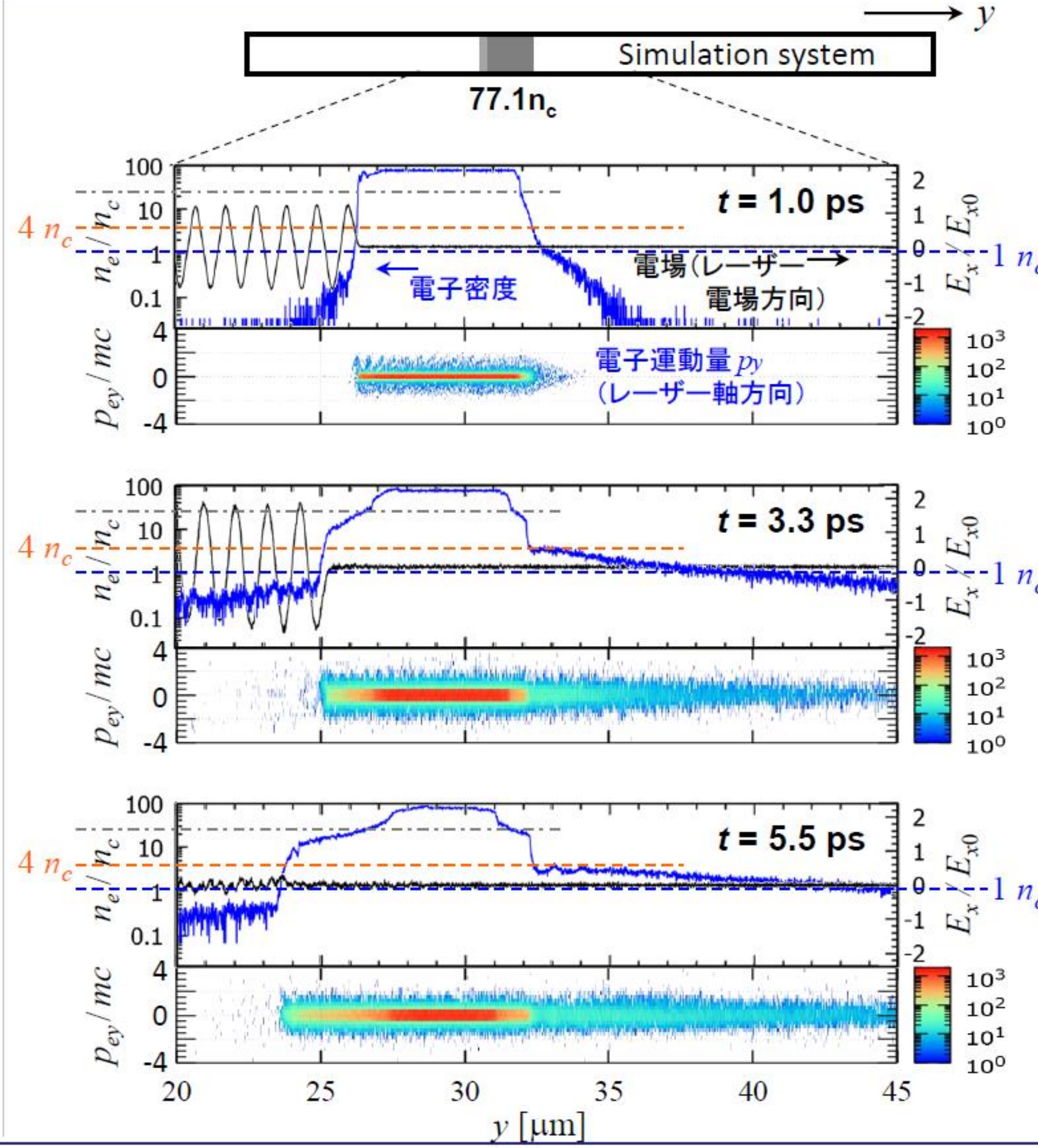

Block diagram of LFEX laser system

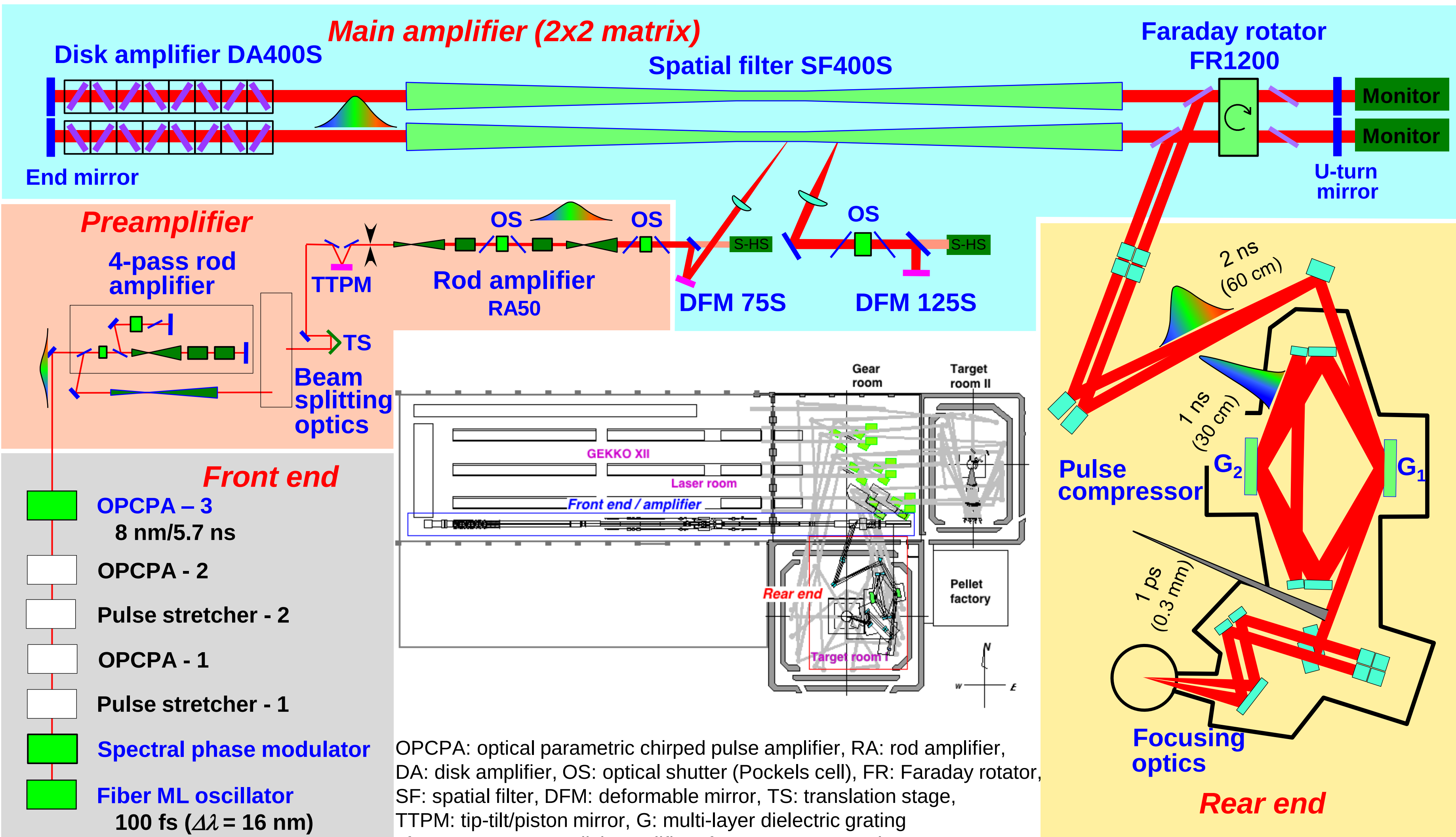

OPCPA: optical parametric chirped pulse amplifier, RA: rod amplifier,
DA: disk amplifier, OS: optical shutter (Pockels cell), FR: Faraday rotator,
SF: spatial filter, DFM: deformable mirror, TS: translation stage,
TTPM: tip-tilt/piston mirror, G: multi-layer dielectric grating
cf. DA400S: square disk amplifier of 400mmx400mm clear aperture

Amplifier components of LFEX laser system

Main disk amp. (2x2)

Faraday rotator (2x2)

Rod amp. (50mm)

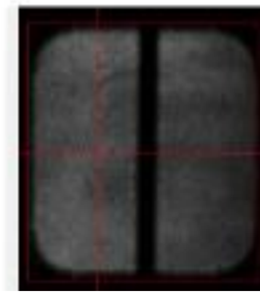

NFP

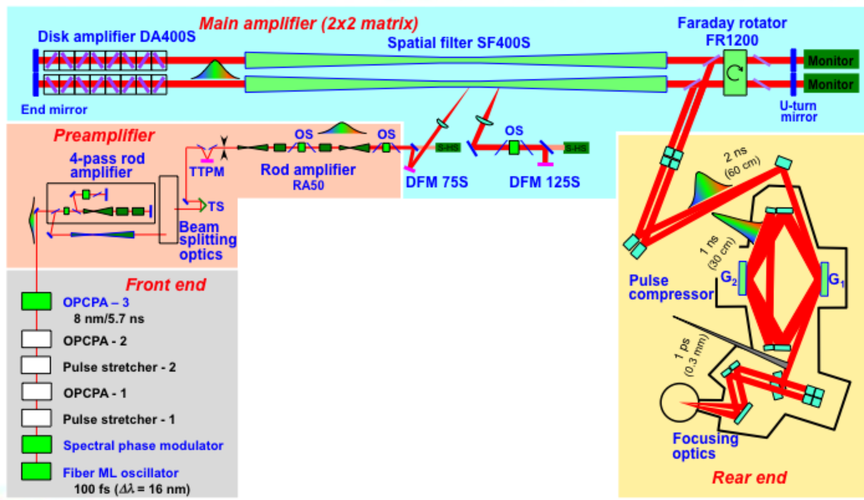

4-pass rod amp. (50mm)

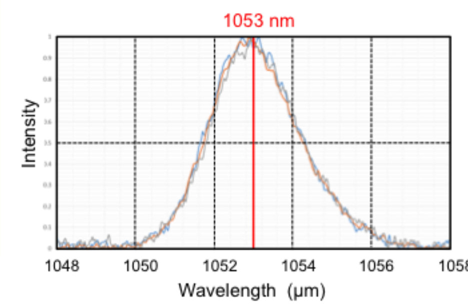

Spectrum

OPCPA

Fiber ML osc.

GVD adjuster

Deformable mirror (75mm, 125mm)

Mechanical structure of rear-end subsystem

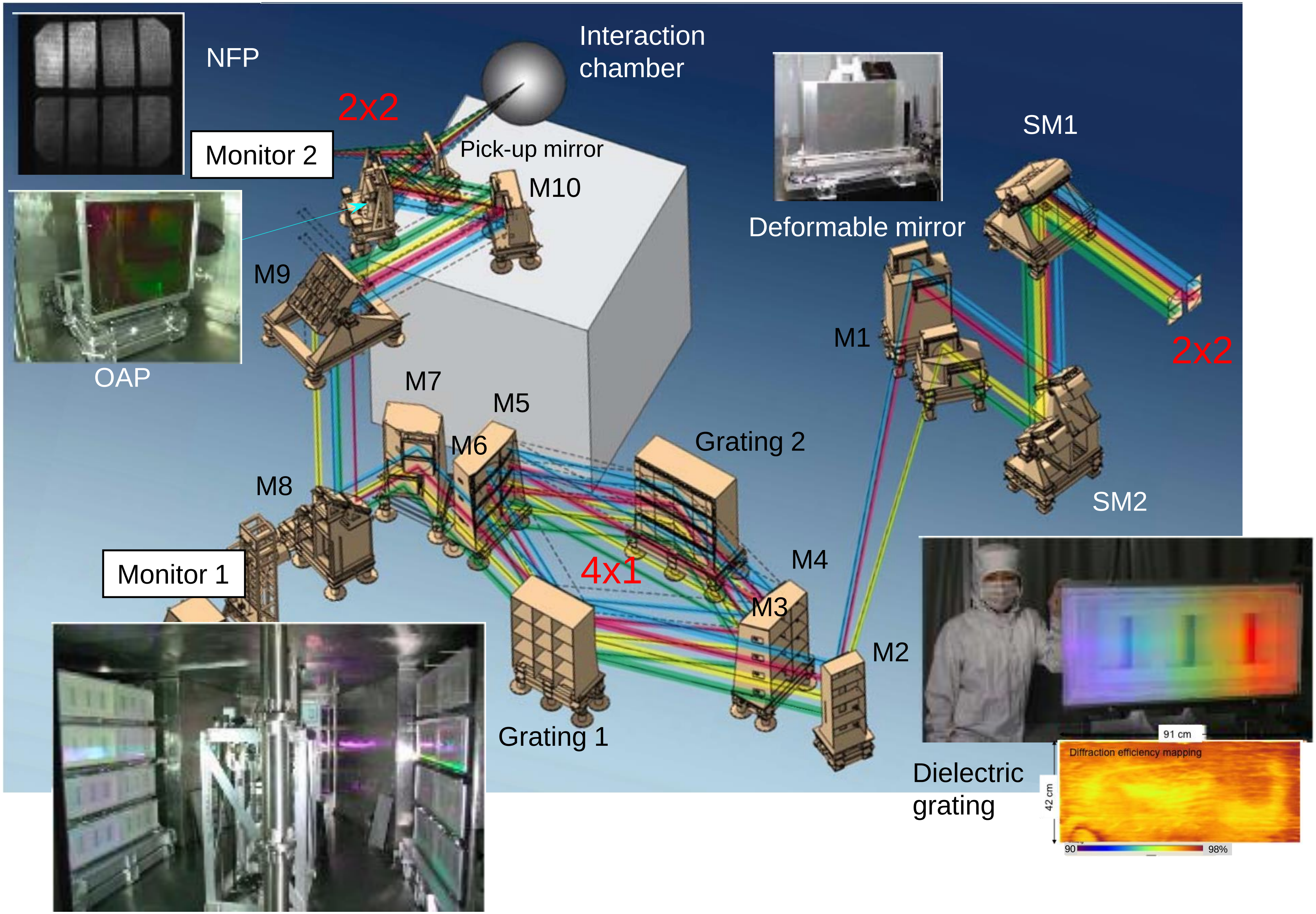

Pulse contrast measurement at the front end

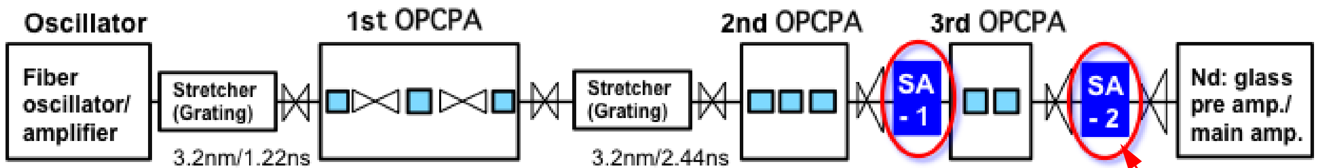

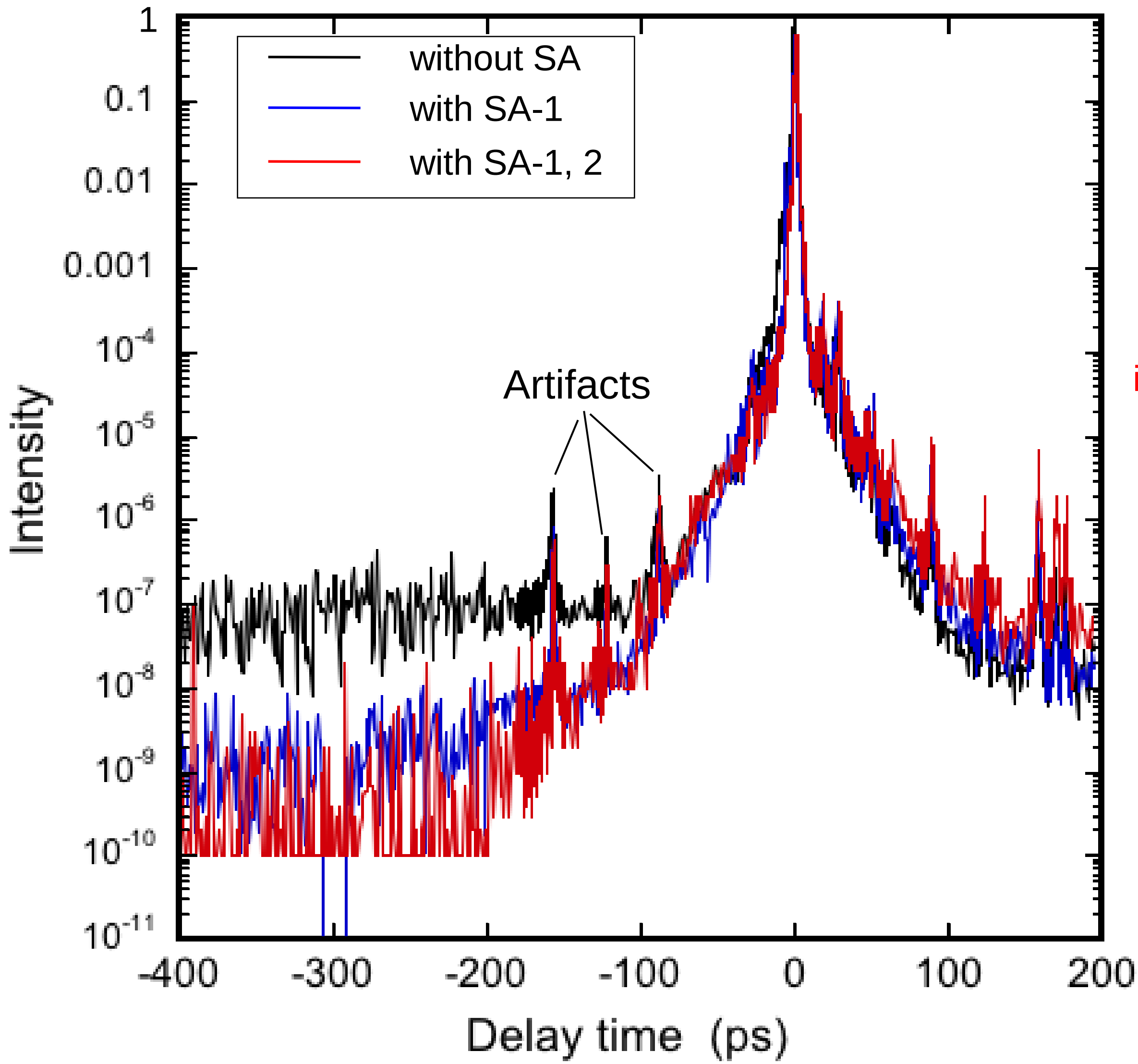

Optical system for pulse contrast improvement using saturable absorber

Dielectric multi-layer grating (40cm × 20cm)

Portable compressor (16-m path length)

Pulse contrast - 1

Deterioration factors of pulse contrast

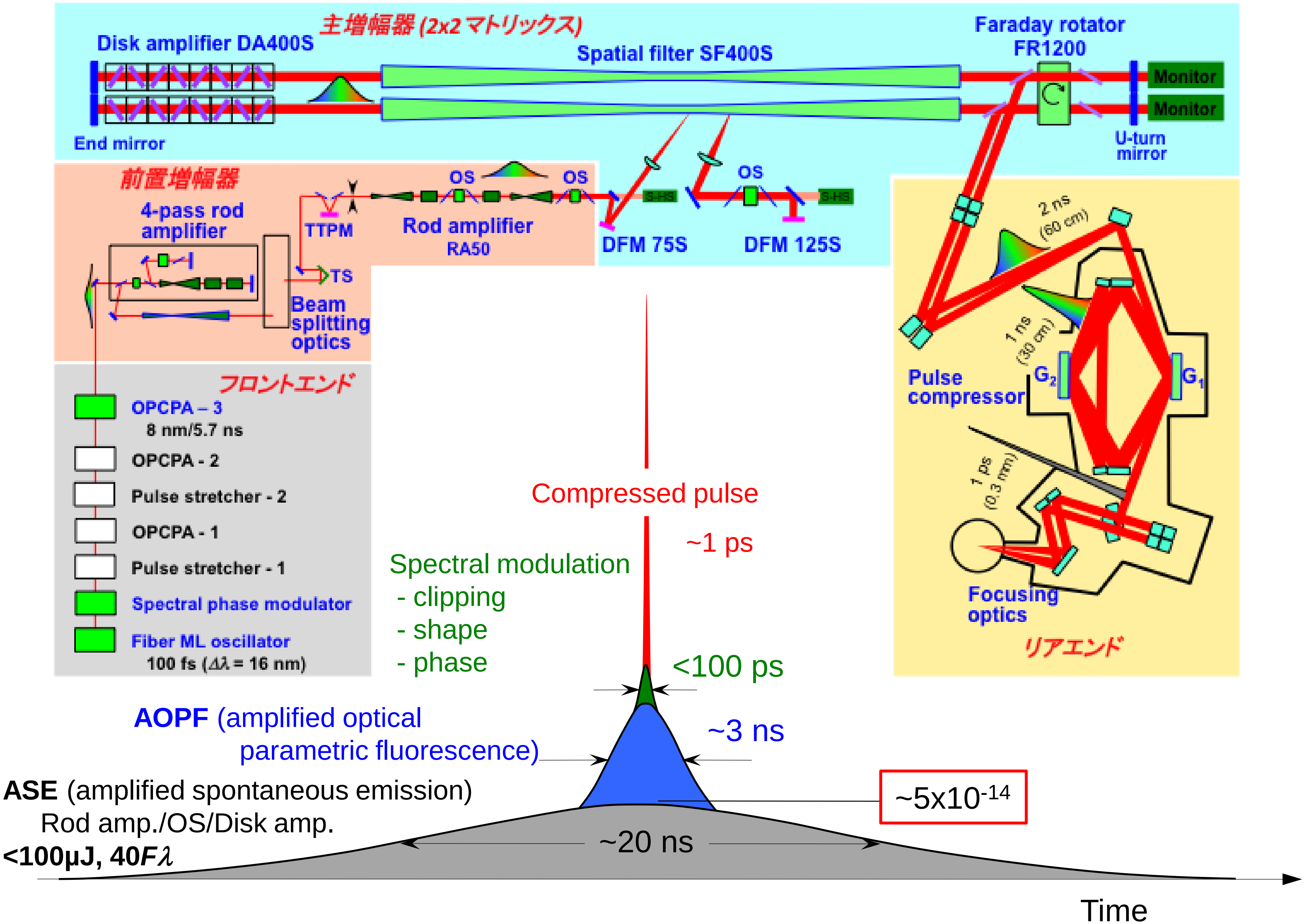

February-March, 2015

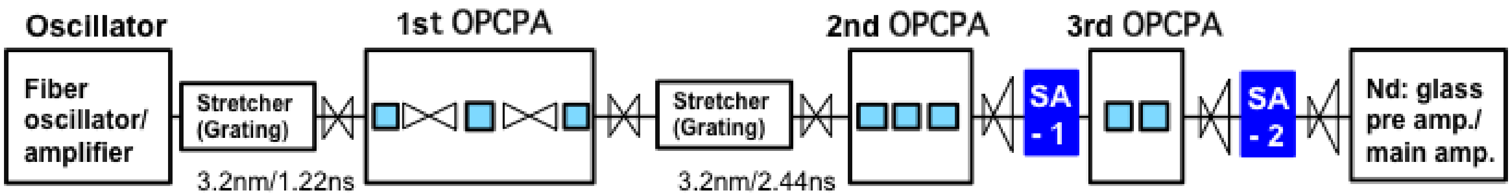

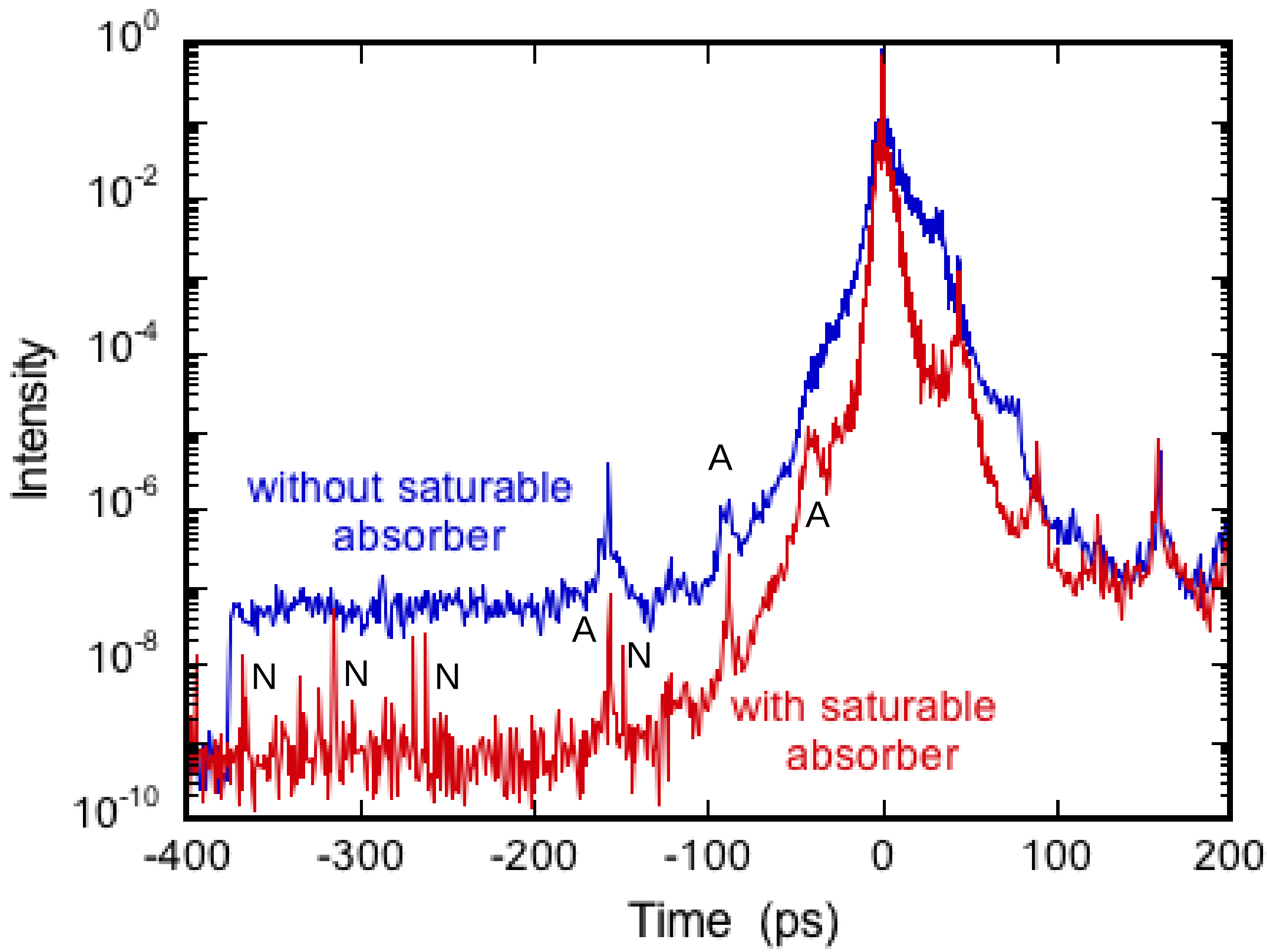

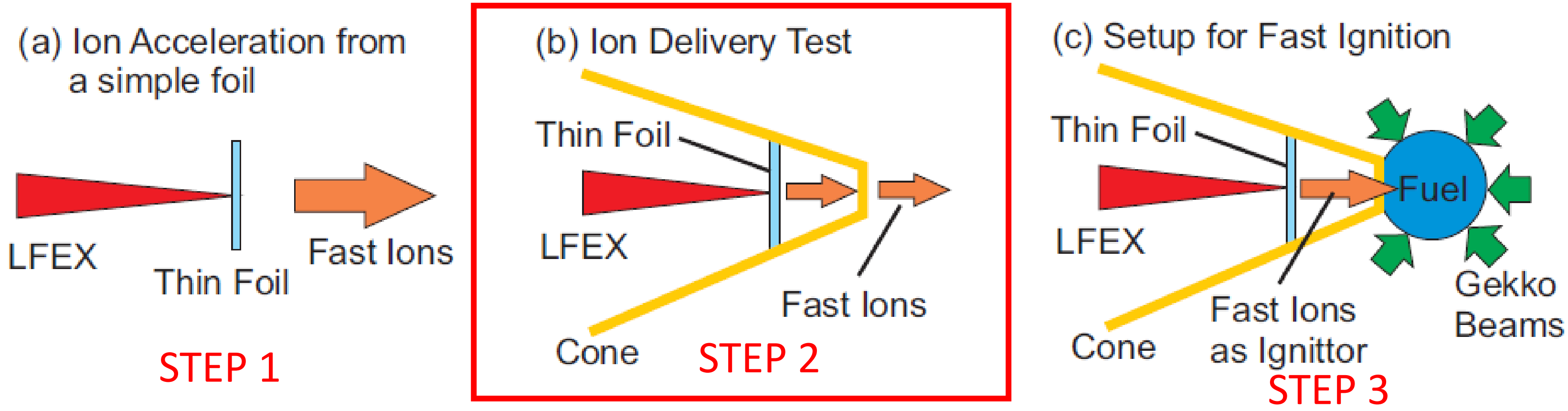

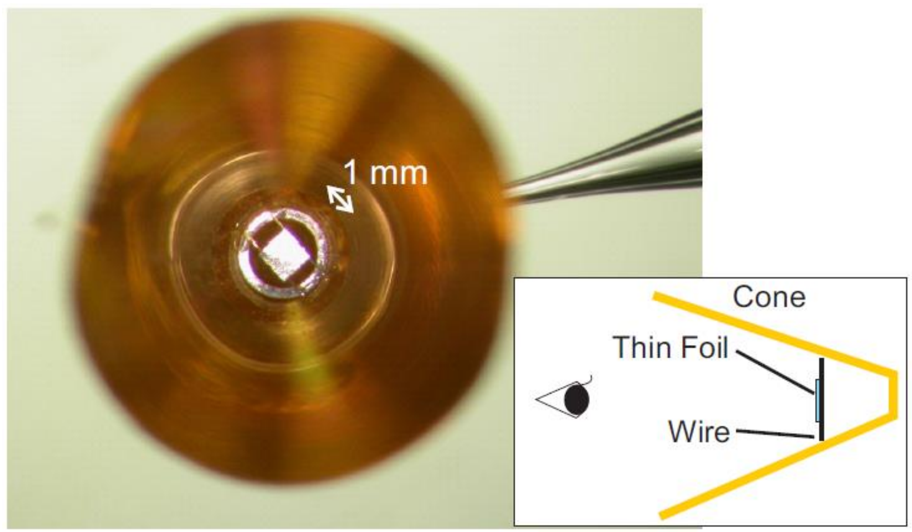

A thin foil target attached inside the cone, developed in ILE, Osaka.